



# Observation of Large CP Violation in the Neutral B Meson System

K. Abe<sup>9</sup>, K. Abe<sup>37</sup>, R. Abe<sup>27</sup>, I. Adachi<sup>9</sup>, Byoung Sup Ahn<sup>16</sup>, H. Aihara<sup>39</sup>, M. Akatsu<sup>20</sup>,  
 G. Alimonti<sup>8</sup>, K. Asai<sup>21</sup>, M. Asai<sup>10</sup>, Y. Asano<sup>44</sup>, T. Asso<sup>43</sup>, V. Aulchenko<sup>2</sup>, T. Aushev<sup>14</sup>,  
 A. M. Bakich<sup>35</sup>, E. Banas<sup>25</sup>, S. Behari<sup>9</sup>, P. K. Behera<sup>45</sup>, D. Beilis<sup>2</sup>, A. Bondar<sup>2</sup>,  
 A. Bozek<sup>25</sup>, T. E. Browder<sup>8</sup>, B. C. K. Casey<sup>8</sup>, P. Chang<sup>24</sup>, Y. Chao<sup>24</sup>, K. F. Chen<sup>24</sup>,  
 B. G. Cheon<sup>34</sup>, R. Chistov<sup>14</sup>, S.-K. Choi<sup>7</sup>, Y. Choi<sup>34</sup>, L. Y. Dong<sup>12</sup>, J. D. Ragic<sup>19</sup>,  
 A. Drutskoy<sup>14</sup>, S. Eidelman<sup>2</sup>, V. Eiges<sup>14</sup>, Y. Enari<sup>20</sup>, R. Enomoto<sup>9</sup>, C. W. Everton<sup>19</sup>,  
 F. Fang<sup>8</sup>, H. Fujii<sup>9</sup>, C. Fukunaga<sup>41</sup>, M. Fukushima<sup>11</sup>, N. Gabyshov<sup>9</sup>, A. Gamashvili<sup>29</sup>,  
 T. J. Gershon<sup>9</sup>, A. Gordon<sup>19</sup>, K. Goto<sup>46</sup>, H. Guler<sup>8</sup>, R. Guo<sup>22</sup>, J. Haba<sup>9</sup>, H. Hamasaki<sup>9</sup>,  
 K. Hanagaki<sup>31</sup>, F. Handa<sup>38</sup>, K. Hara<sup>29</sup>, T. Hara<sup>29</sup>, N. C. Hastings<sup>19</sup>, H. Hayashii<sup>21</sup>,  
 M. Hazumi<sup>29</sup>, E. M. Hoenan<sup>19</sup>, Y. Higashino<sup>20</sup>, I. Higuchi<sup>38</sup>, T. Higuchi<sup>39</sup>, T. Hirai<sup>40</sup>,  
 H. Hirano<sup>42</sup>, T. Hojo<sup>29</sup>, T. Hokuue<sup>20</sup>, Y. Hoshi<sup>37</sup>, K. Hoshina<sup>42</sup>, S. R. Hou<sup>24</sup>, W.-S. Hou<sup>24</sup>,  
 S.-C. Hsu<sup>24</sup>, H.-C. Huang<sup>24</sup>, Y. Igarashi<sup>9</sup>, T. Iijima<sup>9</sup>, H. Ikeda<sup>9</sup>, K. Ikeda<sup>21</sup>, K. Inami<sup>20</sup>,  
 A. Ishikawa<sup>20</sup>, H. Ishino<sup>40</sup>, R. Itoh<sup>9</sup>, G. Iwai<sup>27</sup>, H. Iwasaki<sup>9</sup>, Y. Iwasaki<sup>9</sup>, D. J. Jackson<sup>29</sup>,  
 P. Jalocha<sup>25</sup>, H. K. Jang<sup>33</sup>, M. Jones<sup>8</sup>, R. Kagan<sup>14</sup>, H. Kakuno<sup>40</sup>, J. Kaneko<sup>40</sup>, J. H. Kang<sup>48</sup>,  
 J. S. Kang<sup>16</sup>, P. Kapusta<sup>25</sup>, N. Katayama<sup>9</sup>, H. Kawai<sup>3</sup>, H. Kawai<sup>39</sup>, Y. Kawakami<sup>20</sup>,  
 N. Kawamura<sup>1</sup>, T. Kawasaki<sup>27</sup>, H. Kichim<sup>9</sup>, D. W. Kim<sup>34</sup>, H. Eepong Kim<sup>48</sup>, H. J. Kim<sup>48</sup>,  
 Hyunwoo Kim<sup>16</sup>, S. K. Kim<sup>33</sup>, T. H. Kim<sup>48</sup>, K. Kinoshita<sup>5</sup>, S. Kobayashi<sup>32</sup>, S. Koishi<sup>40</sup>,  
 H. Konishi<sup>42</sup>, K. Korotushenko<sup>31</sup>, P. Kurokovny<sup>2</sup>, R. Kuliasiri<sup>5</sup>, S. Kumar<sup>30</sup>, T. Kuniya<sup>32</sup>,  
 E. Kurihara<sup>3</sup>, A. Kuzmin<sup>2</sup>, Y. J. Kwon<sup>48</sup>, J. S. Lange<sup>6</sup>, G. Leder<sup>13</sup>, M. H. Lee<sup>9</sup>,  
 S. H. Lee<sup>33</sup>, C. Leonidopoulos<sup>31</sup>, Y.-S. Lin<sup>24</sup>, D. Liventsev<sup>14</sup>, R.-S. Lu<sup>24</sup>, J. MacNaughton<sup>13</sup>,  
 D. Marlow<sup>31</sup>, T. Matsubara<sup>39</sup>, S. Matsuji<sup>20</sup>, S. Matsuoto<sup>4</sup>, T. Matsuoto<sup>20</sup>, Y. Miyakawa<sup>38</sup>,  
 K. Misono<sup>20</sup>, K. Miyabayashi<sup>21</sup>, H. Miyake<sup>29</sup>, H. Miyata<sup>27</sup>, L. C. Mott<sup>19</sup>,  
 G. R. Moloney<sup>19</sup>, G. F. Moorhead<sup>19</sup>, S. Mori<sup>44</sup>, T. Mori<sup>4</sup>, A. Muraoka<sup>32</sup>, T. Nagamine<sup>38</sup>,  
 Y. Nagasaka<sup>10</sup>, Y. Nagashima<sup>29</sup>, T. Nakadaira<sup>39</sup>, T. Nakamura<sup>40</sup>, E. Nakano<sup>28</sup>, M. Nakao<sup>9</sup>,  
 H. Nakazawa<sup>4</sup>, J. W. Nam<sup>34</sup>, Z. Natakaniec<sup>25</sup>, K. Neichi<sup>37</sup>, S. Nishida<sup>17</sup>, O. Nitoh<sup>42</sup>,  
 S. Noguchi<sup>21</sup>, T. Nozaki<sup>9</sup>, S. Ogawa<sup>36</sup>, T. Ohshima<sup>20</sup>, Y. Ohshima<sup>40</sup>, T. Okabe<sup>20</sup>,  
 T. Okazaki<sup>21</sup>, S. Okuno<sup>15</sup>, S. L. Olsen<sup>8</sup>, H. Ozaki<sup>9</sup>, P. Pakhlov<sup>14</sup>, H. Palka<sup>25</sup>, C. S. Park<sup>33</sup>,  
 C. W. Park<sup>16</sup>, H. Park<sup>18</sup>, L. S. Peak<sup>35</sup>, M. Peters<sup>8</sup>, L. E. Pihlonen<sup>46</sup>, E. Prebys<sup>31</sup>,  
 J. L. Rodriguez<sup>8</sup>, N. Root<sup>2</sup>, M. Rozanska<sup>25</sup>, K. Rybicki<sup>25</sup>, J. Ryuko<sup>29</sup>, H. Sagawa<sup>9</sup>,  
 Y. Sakai<sup>9</sup>, H. Sakamoto<sup>17</sup>, M. Satapathy<sup>45</sup>, A. Satpathy<sup>9,5</sup>, S. Schrenk<sup>5</sup>, S. Semenov<sup>14</sup>,  
 K. Senyo<sup>20</sup>, Y. Settai<sup>4</sup>, M. E. Sevier<sup>19</sup>, H. Shibuya<sup>36</sup>, B. Shwartz<sup>2</sup>, A. Sidorov<sup>2</sup>, S. Stanic<sup>44</sup>,  
 A. Sugita<sup>20</sup>, A. Sugiyama<sup>20</sup>, K. Sumisawa<sup>9</sup>, T. Sumiyoshi<sup>9</sup>, J.-I. Suzuki<sup>9</sup>, K. Suzuki<sup>3</sup>,  
 S. Suzuki<sup>47</sup>, S. Y. Suzuki<sup>9</sup>, S. K. Swain<sup>8</sup>, H. Tajima<sup>39</sup>, T. Takahashi<sup>28</sup>, F. Takasaki<sup>9</sup>,  
 M. Takita<sup>29</sup>, K. Tamai<sup>9</sup>, N. Tamura<sup>27</sup>, J. Tanaka<sup>39</sup>, M. Tanaka<sup>9</sup>, G. N. Taylor<sup>19</sup>,

Y . Teramoto<sup>28</sup>, M . Tomoto<sup>9</sup>, T . Tomura<sup>39</sup>, S . N . Tovey<sup>19</sup>, K . Trabelsi<sup>8</sup>, T . Tsuboyama<sup>9</sup>,  
T . Tsukamoto<sup>9</sup>, S . Uehara<sup>9</sup>, K . Ueno<sup>24</sup>, Y . Unno<sup>3</sup>, S . Unno<sup>9</sup>, Y . Ushiroda<sup>9</sup>, S . E . Vahsen<sup>31</sup>,  
K . E . Varvell<sup>35</sup>, C . C . Wang<sup>24</sup>, C . H . Wang<sup>23</sup>, J . G . Wang<sup>46</sup>, M . Z . Wang<sup>24</sup>, Y . Watanabe<sup>40</sup>,  
E . Wong<sup>33</sup>, B . D . Yabsley<sup>9</sup>, Y . Yamada<sup>9</sup>, M . Yamaga<sup>38</sup>, A . Yamaguchi<sup>38</sup>, H . Yamamoto<sup>8</sup>,  
T . Yamamoto<sup>29</sup>, Y . Yamashita<sup>26</sup>, M . Yamuchi<sup>9</sup>, S . Yanaka<sup>40</sup>, J . Yashima<sup>9</sup>,  
M . Yokoyama<sup>39</sup>, K . Yoshida<sup>20</sup>, Y . Yusa<sup>38</sup>, H . Yuta<sup>1</sup>, C . C . Zhang<sup>12</sup>, J . Zhang<sup>44</sup>,  
H . W . Zhao<sup>9</sup>, Y . Zheng<sup>8</sup>, V . Zhilich<sup>2</sup>, and D . Zontar<sup>44</sup>

Belle Collaboration

<sup>1</sup> Aomori University, Aomori

<sup>2</sup> Budker Institute of Nuclear Physics, Novosibirsk

<sup>3</sup> Chiba University, Chiba

<sup>4</sup> Chuo University, Tokyo

<sup>5</sup> University of Cincinnati, Cincinnati OH

<sup>6</sup> University of Frankfurt, Frankfurt

<sup>7</sup> Gyeongsang National University, Chinju

<sup>8</sup> University of Hawaii, Honolulu HI

<sup>9</sup> High Energy Accelerator Research Organization (KEK), Tsukuba

<sup>10</sup> Hiroshima Institute of Technology, Hiroshima

<sup>11</sup> Institute for Cosmic Ray Research, University of Tokyo, Tokyo

<sup>12</sup> Institute of High Energy Physics, Chinese Academy of Sciences, Beijing

<sup>13</sup> Institute of High Energy Physics, Vienna

<sup>14</sup> Institute for Theoretical and Experimental Physics, Moscow

<sup>15</sup> Kanagawa University, Yokohama

<sup>16</sup> Korea University, Seoul

<sup>17</sup> Kyoto University, Kyoto

<sup>18</sup> Kyungpook National University, Taegu

<sup>19</sup> University of Melbourne, Victoria

<sup>20</sup> Nagoya University, Nagoya

<sup>21</sup> Nara Women's University, Nara

<sup>22</sup> National Kaohsiung Normal University, Kaohsiung

<sup>23</sup> National Lien-Ho Institute of Technology, Miao Li

<sup>24</sup> National Taiwan University, Taipei

<sup>25</sup> H . Niewodniczanski Institute of Nuclear Physics, Krakow

<sup>26</sup> Nihon Dental College, Niigata

<sup>27</sup> Niigata University, Niigata

<sup>28</sup> Osaka City University, Osaka

<sup>29</sup> Osaka University, Osaka

<sup>30</sup> Panjab University, Chandigarh

<sup>31</sup> Princeton University, Princeton NJ

<sup>32</sup> Saga University, Saga

<sup>33</sup> Seoul National University, Seoul

<sup>34</sup> Sungkyunkwan University, Suwon

<sup>35</sup> University of Sydney, Sydney NSW

<sup>36</sup> Toho University, Funabashi

<sup>37</sup> Tohoku Gakuin University, Tagajo

<sup>38</sup>Tohoku University, Sendai  
<sup>39</sup>University of Tokyo, Tokyo  
<sup>40</sup>Tokyo Institute of Technology, Tokyo  
<sup>41</sup>Tokyo Metropolitan University, Tokyo  
<sup>42</sup>Tokyo University of Agriculture and Technology, Tokyo  
<sup>43</sup>Toyama National College of Marine Technology, Toyama  
<sup>44</sup>University of Tsukuba, Tsukuba  
<sup>45</sup>Utkal University, Bhubaneswar  
<sup>46</sup>Virginia Polytechnic Institute and State University, Blacksburg VA  
<sup>47</sup>Yokkaichi University, Yokkaichi  
<sup>48</sup>Yonsei University, Seoul  
 (January 2, 2019)

## Abstract

We present a measurement of the Standard Model CP violation parameter  $\sin 2\beta_1$  based on a  $29.1 \text{ fb}^{-1}$  data sample collected at the  $(4S)$  resonance with the Belle detector at the KEKB asymmetric-energy  $e^+e^-$  collider. One neutral B meson is fully reconstructed as a  $J = K_S, (2S)K_S, c_1K_S, c_2K_S$ ,  $J = K_L$  or  $J = K^0$  decay and the flavor of the accompanying B meson is identified from its decay products. From the asymmetry in the distribution of the time intervals between the two B meson decay points, we determine  $\sin 2\beta_1 = 0.99 \pm 0.14 \text{ (stat)} \pm 0.06 \text{ (syst)}$ . We conclude that we have observed CP violation in the neutral B meson system.

PACS numbers: 11.30.Er, 12.15.Hh, 13.25.Hw

Kobayashi and Maskawa (KM) proposed, in 1973, a model where CP violation is incorporated as an irreducible complex phase in the weak-interaction quark mixing matrix [1]. The idea, which was presented at a time when only the u, d and s quarks were known to exist, was remarkable because it required the existence of six quarks. The subsequent discoveries of the c, b and t quarks, and the compatibility of the model with the CP violation observed in the neutral K meson system led to the incorporation of the KM mechanism into the Standard Model, even though it had not been conclusively tested experimentally.

In 1981, Sanda, Bigi and Carter [2] pointed out that the KM model predicted large CP violation in certain decays of B mesons for a range of quark mixing parameters. Subsequent measurements of the B meson lifetime [3] and the discovery of  $B^0\bar{B}^0$  mixing [4] indicated that the parameters lie within such a range. Thus, measurements of CP violation in B meson decays provide important tests of the KM model.

The model predicts a CP violating asymmetry in the time-dependent rates for initial  $B^0$  and  $\bar{B}^0$  decays to a common CP eigenstate,  $f_{CP}$  [2]. In the case where  $f_{CP} = (cc)\bar{K}^0$ , the asymmetry is given by

$$A(t) = \frac{(\bar{B}^0 | f_{CP}) - (B^0 | f_{CP})}{(\bar{B}^0 | f_{CP}) + (B^0 | f_{CP})} = f \sin 2\alpha \sin m_d t;$$

where  $(\bar{B}^0 | f_{CP})$  is the decay rate for  $\bar{B}^0(B^0)$  to  $f_{CP}$  at a proper time  $t$  after production,  $f$  is the CP-eigenvalue of  $f_{CP}$ ,  $m_d$  is the mass difference between the two  $B^0$  mass eigenstates, and  $\alpha$  is one of the three internal angles of the Unitarity Triangle, defined as  $\alpha = \arg \frac{V_{tb}V_{td}}{V_{cb}V_{cd}}$  [5]. For the  $(cc)\bar{K}^0$  decays, both the ambiguity due to strong interactions and the contribution from direct CP violation are expected to be small [5].

Our previous determination, using a data sample taken in 1999–2000, found  $\sin 2\alpha = 0.58^{+0.32}_{-0.34} \text{ (stat)}^{+0.09}_{-0.10} \text{ (syst)}$  [6], which is consistent with the KM model constraints from indirect measurements [7]. Although the combination of this result with other measurements of  $\sin 2\alpha$  [8] strongly indicates violation of CP symmetry in B meson decays, the published results are still not conclusive. In this Letter we report a new measurement of  $\sin 2\alpha$  that uses improved reconstruction algorithms and incorporates data taken in 2001 to achieve a four-fold increase in the size of the event sample. The result reported here includes the earlier data and supersedes the previous value.

We use a 29.1  $\text{fb}^{-1}$  data sample, which contains 31.3 million  $B\bar{B}$  pairs, collected with the Belle detector at the KEKB asymmetric-energy  $e^+e^-$  (3.5 on 8 GeV) collider [9]. KEKB operates at the  $(4S)$  resonance ( $\sqrt{s} = 10.58 \text{ GeV}$ ) with a peak luminosity that exceeds  $4 \times 10^{33} \text{ cm}^{-2} \text{ s}^{-1}$ . The Belle detector is a large-solid-angle magnetic spectrometer that consists of a three-layer silicon vertex detector (SVD), a 50-layer central drift chamber (CDC), a mosaic of aerogel threshold Cerenkov counters (ACC), time-of-light scintillation counters (TOF), and an array of CsI(Tl) crystals (ECL) located inside a superconducting solenoid coil that provides a 1.5 T magnetic field. An iron flux-return located outside of the coil is instrumented to detect  $K_L$  mesons and to identify muons (KLM). The detector is described in detail elsewhere [10].

We measure  $\sin 2\alpha$  using  $B^0\bar{B}^0$  meson pairs produced at the  $(4S)$  resonance. The two mesons remain in a coherent p-wave state until one of them decays. The decay of one of the B mesons at time  $t_{tag}$  to a final state,  $f_{tag}$ , which distinguishes between  $B^0$  and  $\bar{B}^0$ , projects the accompanying B meson onto the opposite flavor at  $t_{tag}$ ; this meson decays to  $f_{CP}$  at

time  $t_{CP}$ . CP violation manifests itself as an asymmetry  $A(t)$ , where  $t$  is the proper time interval  $t = t_{CP} - t_{tag}$ . At KEKB, the  $(4S)$  is produced with a Lorentz boost of  $\gamma = 0.425$  nearly along the electron beam line ( $z$ ). Since the  $B^0$  and  $\bar{B}^0$  mesons are nearly at rest in the  $(4S)$  center of mass system (cm s),  $t$  can be determined from the displacement in  $z$  between the  $f_{CP}$  and  $f_{tag}$  decay vertices, i.e.  $t' (z_{CP} - z_{tag}) = c \cdot z = c$ .

The measurement requires the reconstruction of  $B^0 \rightarrow f_{CP}$  decays, the determination of the b-flavor of the accompanying (tagging)  $B$  meson, the measurement of  $t$ , and a fit of the expected  $t$  distribution to the measured distribution using a likelihood method.

We reconstruct  $B^0$  decays to the following CP eigenstates [11]:  $J=K_S$ ,  $(2S)K_S$ ,  $c_1K_S$ ,  $\bar{K}_S$  for  $f = 1$  and  $J=K_L$  for  $f = +1$ . We also use  $B^0 \rightarrow J=K^0 \bar{K}^0$  decays where  $K^0 \bar{K}^0$ . Here the final state is a mixture of even and odd CP, depending on the relative orbital angular momentum of the  $J=$  and  $K^0$ . The CP content is determined from a fit to the full angular distribution of all  $J=K$  decay modes other than  $K^0 \bar{K}_S$ . We find that the final state is primarily  $f = +1$ ; the  $f = -1$  fraction is 0.19 (stat) 0.04 (syst) [12].

$J=$  and  $(2S)$  mesons are reconstructed via their decays to  $\pi^+ \pi^- (\pi^+ \pi^- \eta)$ . The  $(2S)$  is also reconstructed via  $J=K^+$ , and the  $c_1$  via  $J=K^+$ . The  $c_1$  is detected in the  $K^+ K^0$  and  $K_S K^+$  modes. For the  $J=K_S$  mode, we use  $K_S \rightarrow \pi^+ \pi^-$  and  $K_S \rightarrow \pi^0 \pi^0$  decays; for other modes we only use  $K_S \rightarrow \pi^+ \pi^-$ .

The  $J=$ ,  $(2S)$  and  $K_S$  selection has been described elsewhere [6]. For  $c_1 K_S$  decays, we select  $c_1 \rightarrow J=$  decays, rejecting  $\pi$ 's that are consistent with  $K^0 \bar{K}^0$  decays, and use the requirement  $385 < M_{bc} < 430.5$  MeV/c<sup>2</sup>. For  $\bar{K}_S$  decays, we distinguish kaons from pions using a combination of CDC energy loss measurements, flight times measured in the TOF, and the response of the ACC. Candidate  $\bar{K}_S \rightarrow K^+ K^0$  ( $K_S K^+$ ) decays are selected with a  $K K$  mass requirement that takes into account the natural width of the  $c_1$ . For  $J=K^0$  ( $K_S^0$ ) decays, we use  $K_S^0$  combinations that have an invariant mass within 75 MeV/c<sup>2</sup> of the nominal  $K$  mass. We reduce background from low-momentum  $\pi^0$ 's by requiring  $\cos \theta_K < 0.8$ , where  $\theta_K$  is the angle between the  $K_S$  momentum vector and the  $K^0$  flight direction calculated in the  $K^0$  rest frame.

We identify  $B$  decays using the energy difference  $E_B^{\text{cm s}} - E_{\text{beam}}^{\text{cm s}}$  and the beam-energy constrained mass  $M_{bc} = \sqrt{(E_{\text{beam}}^{\text{cm s}})^2 - (p_B^{\text{cm s}})^2}$ , where  $E_{\text{beam}}^{\text{cm s}}$  is the cm s beam energy, and  $E_B^{\text{cm s}}$  and  $p_B^{\text{cm s}}$  are the cm s energy and momentum of the  $B$  candidate.

Figure 1 shows the combined  $M_{bc}$  distribution for all channels other than  $J=K_L$  after a mode-dependent requirement on  $E_B$ . The  $B$  meson signal region is defined as  $5.270 < M_{bc} < 5.290$  GeV/c<sup>2</sup>. Table I lists the numbers of observed candidates ( $N_{\text{ev}}$ ) and the background ( $N_{\text{bkgd}}$ ) determined by extrapolating the rate in the non-signal  $E$  vs.  $M_{bc}$  region into the signal region.

Candidate  $B^0 \rightarrow J=K_L$  decays are selected by requiring ECL and/or KLM hit patterns that are consistent with the presence of a shower induced by a neutral hadron. The centroid of the shower is required to be in a 45° cone centered on the  $K_L$  direction that is inferred from two-body decay kinematics and the measured four-momentum of the  $J=$ . We reduce the background by means of a likelihood ratio that depends on the  $J=$  cm s momentum, the angle between the  $K_L$  and its nearest-neighbor charged track, the charged track multiplicity of the event, the extent to which the event is consistent with a  $B^+ \rightarrow J=K^+ (K_L^+)$  hypothesis, and the polar angle with respect to the  $z$  direction of the reconstructed  $B^0$  meson in the cm s. In addition, we remove events that are reconstructed as

$B^0 \rightarrow J/\psi K_S$ ,  $J/\psi \rightarrow K^+ K^-$ ,  $B^+ \rightarrow J/\psi K^+$ , or  $J/\psi \rightarrow K^+ K^-$  decays. Finally,  $K_L$  clusters with positions that match photons from reconstructed  $\gamma$ 's are also rejected.

Figure 2 shows the  $p_B^{\text{cm}}$  distribution, calculated with the  $B^0 \rightarrow J/\psi K_L$  two-body decay hypothesis. The histograms are the results of a fit to the signal and background distributions. The shapes are derived from Monte Carlo simulations (MC) [13], and the normalization and peak position of the signal are allowed to vary. There are 397 entries in the  $0.2 \leq p_B^{\text{cm}} \leq 0.45$  GeV = c signal region with KLM clusters. There are 172 entries in the range  $0.2 \leq p_B^{\text{cm}} \leq 0.40$  GeV = c with clusters in the ECL only. The fit finds a total of 346  $29 J/\psi K_L$  signal events, and a signal purity of 61%.

Leptons, charged pions, and kaons that are not associated with a reconstructed CP eigenstate decay are used to identify the flavor of the accompanying  $B$  meson. Initially, the b-flavor determination is performed at the track level. Several categories of well-measured tracks that distinguish the b-flavor by the track's charge are selected: high momentum leptons from  $b \rightarrow c \ell^-$ , lower momentum leptons from  $c \rightarrow s \ell^+$ , charged kaons and baryons from  $b \rightarrow c \bar{s}$ , high momentum pions that originate from decays of the type  $B^0 \rightarrow D^{(*)} (\pi^+; \pi^+, \pi^0; \text{etc.})$ , and slow pions from  $D \rightarrow \pi^+ \pi^-$ . We use the MC to determine a category-dependent variable that indicates whether a track originates from a  $B^0$  or  $\bar{B}^0$ . The values of this variable range from -1 for a reliably identified  $\bar{B}^0$  to +1 for a reliably identified  $B^0$  and depend on the tagging particle's charge, momentum, polar angle and particle-identification probability, as well as other kinematic and event shape quantities. The results from the separate track categories are then combined to take into account correlations in the case of multiple track-level tags. This stage determines two event-level parameters,  $q$  and  $r$ . The first,  $q$ , has the discrete values  $q = +1$  when the tag-side  $B$  meson is more likely to be a  $B^0$  and -1 when it is more likely to be a  $\bar{B}^0$ . The parameter  $r$  is an event-by-event flavor-tagging dilution factor which ranges from  $r = 0$  for no flavor discrimination to  $r = 1$  for unambiguous flavor assignment. It is used only to sort data into six intervals of  $r$ , according to flavor purity; the wrong-tag probabilities for the final fit are determined from data.

The probabilities of an incorrect flavor assignment,  $w_1$  ( $l = 1; 6$ ), are determined directly from the data for the six  $r$  intervals using exclusively reconstructed, self-tagged  $B^0 \rightarrow D^{(*)} \pi^+$ ,  $D^{(*)} \pi^0$ , and  $J/\psi K^0$  decays. The b-flavor of the accompanying  $B$  meson is assigned according to the flavor-tagging algorithm described above. The exclusive decay and tag vertices are reconstructed using the same vertexing algorithm that is used in the analysis to measure CP asymmetry. The values of  $w_1$  are obtained from the amplitudes of the time-dependent  $B^0 \bar{B}^0$  mixing oscillations:  $(N_{OF} - N_{SF}) = (N_{OF} + N_{SF}) = (1 - 2w_1) \cos(\Delta m d t)$ . Here  $N_{OF}$  and  $N_{SF}$  are the numbers of opposite and same flavor events. We fix  $m_d$  at the world average value [14]. Table II lists the resulting  $w_1$  values together with the fraction of the events ( $f_1$ ) in each  $r$  interval. The total effective tagging efficiency is  $\sum_1^6 f_1 (1 - 2w_1)^2 = 0.270 \pm 0.008 \text{ (stat)} \pm 0.009 \text{ (syst)}$ .

The vertex positions for the  $f_{CP}$  and  $f_{tag}$  decays are reconstructed using tracks that have at least one three-dimensional coordinate determined from associated  $r$ - and  $z$  hits in the same SVD layer along with one or more additional  $z$  hits in the other layers. Each vertex position is required to be consistent with the interaction point profile smeared in the  $r$ -plane by the  $B$  meson decay length. The  $f_{CP}$  vertex is determined using lepton tracks from

$J=$  or  $(2S)$  decays, or prompt tracks from  $c$  decays. The  $f_{tag}$  vertex is determined from well reconstructed tracks not assigned to  $f_{CP}$ . Tracks that form a  $K_S$  are not used. The MC indicates that the typical vertex- finding efficiency and vertex resolution (in  $\text{m s}$ ) for  $z_{CP}$  ( $z_{tag}$ ) are 92 (91)% and 75 (140)  $\text{m}$ , respectively.

The proper time interval resolution for the signal,  $R_{sig}(t)$ , is obtained by convolving a sum of two Gaussians (a main component due to the SVD vertex resolution and charmed meson lifetimes, plus a tail component caused by poorly reconstructed tracks) with a function that takes into account the motion of the  $B$  mesons. The fraction in the main Gaussian is determined to be 0.97 ± 0.02 from a study of  $B^0 \rightarrow D^+ \bar{D}^0 \rightarrow D^+ \pi^-$ ,  $J=K^0$ ,  $J=K_S$  and  $B^+ \rightarrow \bar{D}^0 \pi^+$ ,  $J=K^+$  events. The means ( $_{\text{main}}$ ,  $_{\text{tail}}$ ) and widths ( $_{\text{main}}$ ,  $_{\text{tail}}$ ) of the Gaussians are calculated event-by-event from the  $f_{CP}$  and  $f_{tag}$  vertex  $t$  error matrices and the  $\chi^2$  values of the  $t$ ; typical values are  $_{\text{main}} = 0.24 \text{ ps}$ ,  $_{\text{tail}} = 0.18 \text{ ps}$  and  $_{\text{main}} = 1.49 \text{ ps}$ ,  $_{\text{tail}} = 3.85 \text{ ps}$ . The background resolution  $R_{bkg}(t)$  has the same functional form but the parameters are obtained from a sideband region in  $M_{bc}$  and  $E$ . We obtain lifetimes for the neutral and charged  $B$  mesons using the same procedure; the results [15] agree well with the world average values.

After vertexing we find 560 events with  $q_f = +1$  flavor tags and 577 events with  $q_f = -1$ . Figure 3 shows the observed  $t$  distributions for the  $q_f = +1$  (solid points) and  $q_f = -1$  (open points) event samples. There is a clear asymmetry between the two distributions; this demonstrates that CP symmetry is violated.

We determine  $\sin 2\beta_1$  by performing an unbinned maximum-likelihood fit of a CP violating probability density function (pdf) to the observed  $t$  distributions. For modes other than  $J=K^0$  the pdf expected for the signal is

$$P_{sig}(t; q_f; w_1; f) = \frac{e^{j t \frac{m_d}{m_B} B^0}}{2 \pi B^0} f_1 - f_2 q_f (1 - 2w_1) \sin 2\beta_1 \sin(m_d t) g;$$

where we set  $m_d$  and  $m_B$  at their world average values [14]. The pdf used for the background distribution is  $P_{bkg}(t) = f_b e^{j t \frac{m_d}{m_B} B^0} = f_b g + (1 - f_b) \delta(t)$ ; where  $f_b$  is the fraction of the background component with an effective lifetime  $\tau_{bkg}$  and  $\delta$  is the Dirac delta function. For all  $f_{CP}$  modes other than  $J=K_L$ , a study using events in background-dominated regions of  $E$  vs.  $M_{bc}$  shows that  $f_b$  is negligibly small. For these modes,  $P_{bkg}(t) = g(t)$ .

The  $J=K_L$  background is dominated by  $B^0 \rightarrow J=K_L$  decays where some final states are CP eigenstates. We estimate the fractions of the background components with and without a true  $K_L$  cluster by fitting the  $p_T^m$  distribution to the expected shapes determined from the MC. We also use the MC to determine the fraction of events with definite CP content within each component.

The result is a background that is 71% non-CP modes with  $f_{bkg} = f_B$ . For the CP-m mode backgrounds we use the signal pdf given above with the appropriate  $f$  values. For  $J=K_L$  ( $K_L^0$ ), which is 13% of the background, we use the  $f_f = 1$  content determined from the full  $J=K_L$  sample. The remaining backgrounds are  $f_f = 1$  states (10%) including  $J=K_S$ , and  $f_f = +1$  states (5%) including  $(2S)K_L$ ,  $c\bar{c}K_L$  and  $J=K^0$ .

For the  $J=K_L$  mode, we include the  $t$  and transversity angle  $\chi_T$  [16] distributions in the likelihood [12]. We use the  $f_f$  content determined from the full angular analysis.

Each pdf is convolved with the appropriate  $R(t)$  to determine the likelihood value for

each event as a function of  $\sin 2 \Delta_1$ :

$$P_i = \sum_z f_{sig} P_{sig}(t^0; q; w_1; f) R_{sig}(t - t^0) + (1 - f_{sig}) P_{bkg}(t^0) R_{bkg}(t - t^0) g d t^0;$$

where  $f_{sig}$  is the probability that the event is signal, calculated as a function of  $p_B^{cm}$  for  $J = K_L$  and of  $E$  and  $M_{bc}$  for other modes. The only free parameter is  $\sin 2 \Delta_1$ , which is determined by maximizing the likelihood function  $L = \prod_i P_i$ , where the product is over all events.

The result of the fit is

$$\sin 2 \Delta_1 = 0.99 \pm 0.14 \text{ (stat)} \pm 0.06 \text{ (syst)};$$

In Fig. 4(a) we show the asymmetries for the combined data sample that are obtained by applying the fit to the events in each  $t$  bin separately. The smooth curve is the result of the global unbinned fit. Figures 4(b) and (c) show the corresponding asymmetries for the  $(\bar{c}c)K_S$  ( $f = -1$ ) and the  $J = K_L$  ( $f = +1$ ) modes separately. The observed asymmetries for the different CP states are opposite, as expected. The curves are the results of unbinned fits applied separately to the two samples; the resultant  $\sin 2 \Delta_1$  values are  $0.84 \pm 0.17$  (stat) and  $1.31 \pm 0.23$  (stat), respectively.

The systematic error is dominated by uncertainties due to effects of the tails of the vertex distributions, which contribute 0.04. Other significant contributions come from uncertainties (a) in  $w_1$  (0.03); (b) in the resolution function parameters (0.02); and (c) in the  $J = K_L$  background fraction (0.02). The errors introduced by uncertainties in  $m_d$  and  $m_{B^0}$  are 0.01 or less.

We performed a number of checks on the measurement. Table III lists the results obtained by applying the same analysis to various subsamples. All values are statistically consistent with each other. The result is unchanged if we use the  $w_1$ 's determined separately for  $f_{tag} = B^0$  and  $\bar{B}^0$ . Fitting to the non-CP eigenstate self-tagged modes  $B^0 \rightarrow D^0 \pi^+$ ,  $D^+ \pi^+$ ,  $J = K^0 (K^+ \pi^-)$  and  $D^+ \pi^+$ , where no asymmetry is expected, yields  $0.05 \pm 0.04$ . The asymmetry distribution for this control sample is shown in Fig. 4(d). As a further check, we used three independent CP fitting programs and two different algorithms for the  $f_{tag}$  vertexing and found no discrepancy.

We conclude that there is large CP violation in the neutral  $B$  meson system. A zero value for  $\sin 2 \Delta_1$  is ruled out at a level greater than 6%. Our result is consistent with the higher range of values allowed by the constraints of the KM model as well as with our previous measurement.

We wish to thank the KEKB accelerator group for the excellent operation of the KEKB accelerator. We acknowledge support from the Ministry of Education, Culture, Sports, Science and Technology of Japan and the Japan Society for the Promotion of Science; the Australian Research Council and the Australian Department of Industry, Science and Resources; the Department of Science and Technology of India; the BK21 program of the Ministry of Education of Korea and the Center for High Energy Physics sponsored by the KOSEF; the Polish State Committee for Scientific Research under contract No 2P03B 17017; the Ministry of Science and Technology of Russian Federation; the National Science Council and the Ministry of Education of Taiwan; and the U.S. Department of Energy.

## REFERENCES

- [1] M. Kobayashi and T. Maskawa, *Prog. Theor. Phys.* **49**, 652 (1973).
- [2] A.B. Carter and A.I. Sanda, *Phys. Rev. D* **23**, 1567 (1981); I.I. Bigi and A.I. Sanda, *Nucl. Phys. B* **193**, 85 (1981).
- [3] E. Fernandez et al. (MAC Collab.), *Phys. Rev. Lett.* **51**, 1022 (1983); N. Lockyer et al. (Mark II Collab.), *Phys. Rev. Lett.* **51**, 1316 (1983).
- [4] H. Albrecht et al. (ARGUS Collab.), *Phys. Lett. B* **192**, 245 (1987).
- [5] H. Quinn and A.I. Sanda, *Eur. Phys. Jour. C* **15**, 626 (2000). (This angle is also known as  $\alpha$ .)
- [6] A. Abashian et al. (Belle Collab.), *Phys. Rev. Lett.* **86**, 2509 (2001).
- [7] For example: M. Ciuchini et al., [hep-ph/0012308](#), submitted for publication to JHEP.
- [8] B. Aubert et al. (BaBar Collab.), *Phys. Rev. Lett.* **86**, 2515 (2001) reports  $\sin 2\alpha = 0.34 \pm 0.20 \pm 0.05$ ; T. Alexander et al. (CDF Collab.), *Phys. Rev. D* **61**, 072005 (2000) reports  $\sin 2\alpha = 0.79^{+0.41}_{-0.44}$ ; R. Barate et al. (ALEPH Collab.), *Phys. Lett. B* **492**, 259 (2000) reports  $\sin 2\alpha = 0.84^{+0.82}_{-1.04} \pm 0.16$ ; and K. Ackersta et al. (OPAL Collab.), *Eur. Phys. Jour. C* **5**, 379 (1998) reports  $\sin 2\alpha = 3.2^{+1.8}_{-2.0} \pm 0.5$ .
- [9] KEKB B Factory Design Report, KEK Report 95-1, 1995, unpublished.
- [10] K. Abe et al. (Belle Collab.), The Belle Detector, KEK Report 2000-4, to be published in *Nucl. Instrum. Methods*.
- [11] Throughout this Letter, whenever a mode is quoted the inclusion of the charge conjugate mode is implied.
- [12] K. Abe et al. (Belle Collab.), Measurements of Polarization and CP Asymmetry in  $B \rightarrow J/\psi + K$  decays, paper submitted to LP01, Rome, July 2001; BELLE-CONF-0105.
- [13] We use the  $Q\bar{Q}$  B meson decay event generator developed by the CLEO Collaboration (<http://www.lns.cornell.edu/public/CLEO/soft/QQ>) and GEANT3 for the detector simulation; CERN Program Library Long Writeup W 5013, CERN, 1993.
- [14] D. E. Groom et al. (Particle Data Group), *Eur. Phys. J. C* **15**, 1 (2000).
- [15] The measured B-lifetimes are:  $B^0 = 1.547 \pm 0.021$  ps and  $B^+ = 1.641 \pm 0.033$  ps (statistical errors only).
- [16]  $\alpha$  is defined as the angle between the  $J/\psi$  direction in the  $J/\psi$  rest frame and the z-axis, where the x-axis is defined as the direction of motion of the  $J/\psi$  in the (4S) rest frame. The x-y plane is defined by the  $K^+$  decay products in the  $J/\psi$  rest frame.

TABLE I. The numbers of observed events ( $N_{ev}$ ) and the estimated background ( $N_{bkgd}$ ) in the signal region for each  $f_{CP}$  mode.

Mode	$N_{ev}$	$N_{bkgd}$
$J = (\pi^+ \pi^-) K_S (\pi^+ \pi^-)$	457	11.9
$J = (\pi^+ \pi^-) K_S (\pi^0 \pi^0)$	76	9.4
$(2S)(\pi^+ \pi^-) K_S (\pi^+ \pi^-)$	39	1.2
$(2S)(J = \pi^+ \pi^-) K_S (\pi^+ \pi^-)$	46	2.1
$c\bar{c}(J = \pi^+ \pi^-) K_S (\pi^+ \pi^-)$	24	2.4
$c\bar{c}(K^+ K^-) K_S (\pi^+ \pi^-)$	23	11.3
$c\bar{c}(K_S K_L) (\pi^+ \pi^-)$	41	13.6
$J = K^0 (\bar{K}_S^0)$	41	6.7
Sub-total	747	58.6
$J = (\pi^+ \pi^-) K_L$	569	223

TABLE II. The event fractions ( $f_1$ ) and incorrect flavor assignment probabilities ( $w_1$ ) for each  $r$  interval. The errors include both statistical and systematic uncertainties.

l	r	$f_1$	$w_1$
1	0:000	0.250	$0.465^{+0.010}_{-0.009}$
2	0.250	0.500	$0.352^{+0.015}_{-0.014}$
3	0.500	0.625	$0.243^{+0.021}_{-0.030}$
4	0.625	0.750	$0.176^{+0.022}_{-0.017}$
5	0.750	0.875	$0.110^{+0.022}_{-0.014}$
6	0.875	1:000	$0.041^{+0.011}_{-0.010}$

TABLE III. The values of  $\sin 2\theta_1$  for various subsamples (statistical errors only).

Sample	$\sin 2\theta_1$
$f_{tag} = B^0$ ( $q = +1$ )	0.84 0.21
$f_{tag} = \bar{B}^0$ ( $q = -1$ )	1.11 0.17
$J = K_S (\pi^+ \pi^-)$	0.81 0.20
$(cc)K_S$ except $J = K_S (\pi^+ \pi^-)$	1.00 0.40
$J = K_L$	1.31 0.23
$J = K^0 (\bar{K}_S^0)$	0.85 1.45
All	0.99 0.14

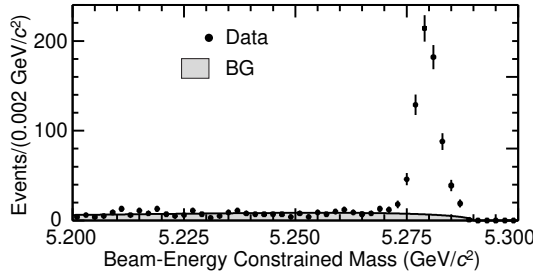


FIG .1. The beam -energy constrained mass distribution for all decay m odes combined other than  $J= K_L$ . The shaded area is the estimated background. The signal region is the range  $5.27 - 5.29$   $\text{GeV}/c^2$ .

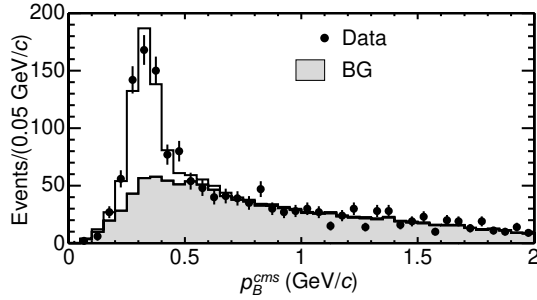


FIG .2. The  $p_B^{\text{cm}\text{s}}$  distribution for  $B^0 \rightarrow J= K_L$  candidates w ith the results of the  $t$ . The solid line is the signal plus background; the shaded area is background only. The signal region for K LM (ECL-only) clusters is  $0.2 < p_B^{\text{cm}\text{s}} < 0.45$  ( $0.40$ )  $\text{GeV}=c$ .

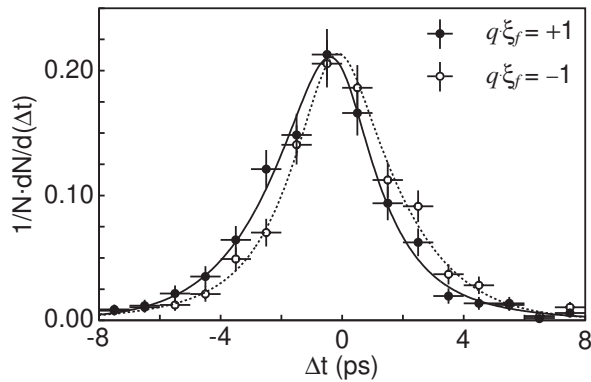


FIG .3.  $t$  distributions for the events w ith  $q_f = +1$  (solid points) and  $q_f = -1$  (open points). The results of the global  $t$  (w ith  $\sin 2\xi_1 = 0.99$ ) are shown as solid and dashed curves, respectively.

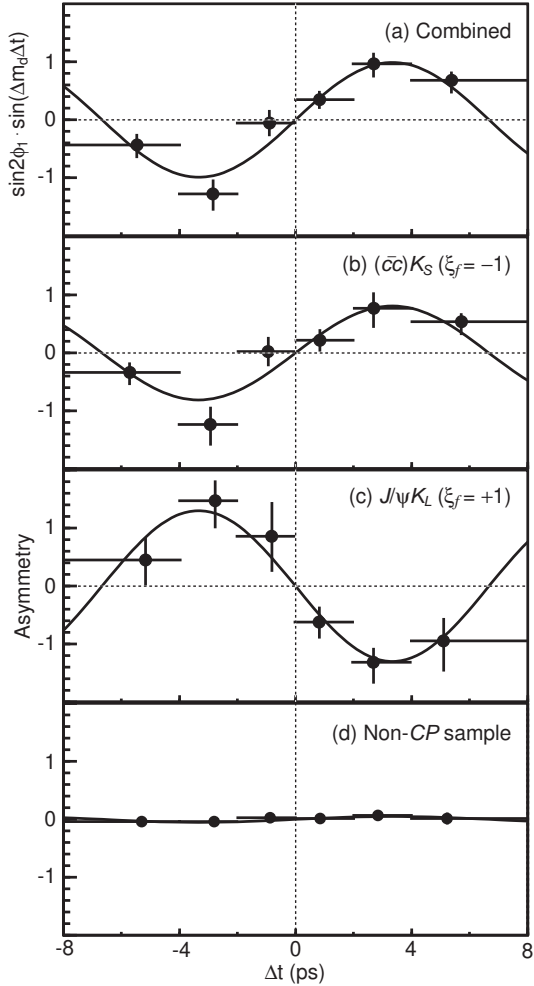


FIG . 4. (a) The asymmetry obtained from separate fits to each  $\Delta t$  bin for the full data sample; the curve is the result of the global fit. The corresponding plots for the (b)  $(cc)K_S$  ( $\xi_f = -1$ ), (c)  $J/\psi K_L$  ( $\xi_f = +1$ ), and (d)  $B^0$  control samples are also shown. The curves are the results of the fits applied separately to the individual data samples.